Multidiszciplináris Tudományok, 14. kötet, 3. szám (2024) pp. 168-176. **https://doi.org/10.35925/j.multi.2024.3.15**

NUMERICAL MODELING OF SINGLE-POINT INCREMENTAL SHEET METAL FORMING OF 3003-O ALUMINUM ALLOY

Marwen Habbachi
PhD student, Institute of Applied Mechanics, University of Miskolc
3515 Miskolc, Miskolc-Egyetemváros, e-mail: marwen.habbachi@student.uni-miskolc.hu

Attila Baksa
associate professor, Institute of Applied Mechanics, University of Miskolc
3515 Miskolc, Miskolc-Egyetemváros, e-mail: attila.baksa@uni-miskolc.hu

Abstract

Incremental sheet metal forming processes have demonstrated promising results in shaping symmetric, asymmetric, and highly complex forms. Their flexibility and reliability have garnered attention across various application areas. In this research, numerical modeling was conducted to investigate incremental sheet metal forming processes, particularly single-point incremental forming (SPIF). An aluminum sheet was used in the forming process. The results were compared with experimental data, showing reasonable agreement. The forming force in the out-of-plane direction was significantly higher than the forming force components in the x- and y-axes. Additionally, it was found that the stress distribution exhibited an asymmetric evolution.

Keywords: *Numerical modeling, incremetal sheet metal forming (ISF), step depth, aluminum alloy Al 3003.*

1. Introduction

Incremental sheet metal forming processes (ISF) have gained recognition among researchers as a viable alternative to conventional methods due to their ability to shape highly complex forms, both symmetric and asymmetric. This technique offers numerous advantages such as short lead time, cost-effectiveness, facilitation of rapid prototyping, and suitability for low production rate (Jeswiet et al., 2005). It has garnered significant attention from the engineering community (Jeswiet et al., 2005; Ambrogio et al., 2012). This innovative approach involves gradually deforming a fixed sheet along its edges by moving a forming tool along a prescribed toolpath controlled by a CNC machine. Figure 1 illustrates the main components of this process, where the clamping plate secures the part at its periphery, and the forming tool and full die determine the geometry of the final product. Unlike conventional methods, ISF does not require dedicated tools for three-dimensional shaping (Wang et al., 2017). Localized deformation has been identified as the primary mechanism for incremental forming, elucidated during the initial stages of its development. Much research has focused on forming strategies and process modeling to enhance our understanding of deformation mechanics (Hirt et al., 2004). ISF allows sheets to stretch beyond the forming limit curves (FLC) observed in traditional processes like deep drawing and stamping, owing to localized incremental plastic deformation (Jeswiet et al., 2005; Filice et al., 2002). However, ISF faces limitations such as extended processing times, making it more suitable for small series and customized products as discussed elsewfhere (Mezher et al., 2018; Paniti et al., 2020; Trzepieciński et al., 2022). Additionally, challenges include compromised geometrical accuracy and

surface quality (Li et al., 2015; Hirt et al., 2004). Several studies have explored the reliability of ISF compared to conventional methods, highlighting improvements in formability (Tisza et al., 2013). These enhancements are attributed to thermal softening, resulting in greater elongation, as well as significant reductions in forming force compared to deep drawing. Moreover, the flexibility of ISF allows for the use of free roller end-mill tools with hemispherical or flat end-mill shapes to further enhance formability (Li et al., 2014).

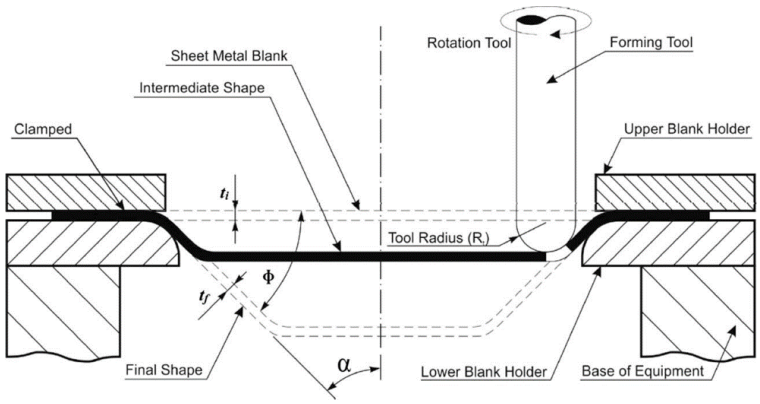

Figure 1. *Single point incremental sheet metal forming mechanism (Gatea et al., 2016)*

In the current research work, a finite element simulation has been developed to investigate single-point incremental forming of aluminum alloy sheet Al 3003-O. Aim to study the forming force behavior and its evolution with forming time, the stress distribution in a plane parallel to the tool direction.

2. Material properties of aluminum alloy Al 3003-O

In this research, we focused on investigating an aluminum alloy, specifically Al 3003-O in its annealed condition, due to its notable characteristics of high ductility, weldability, and corrosion resistance. These properties make it a preferred choice for a wide range of applications, including food and chemical handling equipment, tanks, trims, vessels, pressure components, and piping. Table 1 provides the chemical composition of this aluminum alloy grade, offering insights into its elemental makeup and ensuring a comprehensive understanding of its material properties. With an ultimate strength ranging between 95 and 135 MPa, and a specified proof yielding of 35 MPa, the material exhibits considerable strength while maintaining a high level of ductility. Based on a 50 mm initial gage, the predicted elongation of this material reaches 17%, as specified by the supplier's catalog. Additionally, the elastic modulus of the material is measured at 70000 MPa, indicating its ability to deform under stress while returning to its original shape once the stress is removed. The Poisson's ratio, denoted as ν, is calculated to be 0.33, providing insights into the material's response to tensile and compressive loads. To model the material behavior accurately, a Swift hardening law expression was employed ($Equation$ (1)) to describe the stress-strain relationship as indicated by Habbachi et al. (2024):

$$\sigma = k(\varepsilon + \varepsilon_0)^n \tag{1}$$

where σ represents stress, ε denotes strain, and the parameters k, ε_0, and n govern the material's strain hardening behavior. With a strength coefficient (k) of 183 MPa and a pre-strain value (ε_0) of 5.7×10^{-4}, the material exhibits a strain hardening exponent (n) of 0.229. Furthermore, the Lankford

anisotropy coefficients of the sample material were considered in the numerical simulations, as presented in Table 2. These coefficients provide crucial insights into the material's directional deformation behavior, allowing for a more accurate representation of its response to forming processes. By incorporating these detailed material properties and parameters into our investigation, we aimed to enhance the accuracy and reliability of our numerical simulations, providing valuable insights into the behavior of Al 3003-O during single-point incremental forming processes.

Table 1. *Chemical composition of Al 3003-O*

Element	Al	Cu	Fe	Mn	Si	Zn	Other
Weight (%)	96.7 - 99	0.05 - 0.20	<= 0.70	1.0 - 1.5	<= 0.60	<= 0.10	<= 0.15

Table 2. *Anisotropy coefficients of Al 3003-O*

Anisotropy coefficients	r_0	r_{45}	r_{90}
Values	0.68067	1.184647	0.6639

3. Tool path generation

The choice of toolpath strategy plays a pivotal role in shaping the behavior of forming forces, thinning characteristics, and surface roughness in the deformed sheet. In our investigation, we opted for a spiral toolpath to create a truncated cone shape, utilizing standard parameters for precise control and reproducibility. Specifically, the tool diameter was set to $d = 12.7$ mm, the step size to $\Delta z = 0.5$ mm, the wall angle fixed at $\Phi = 50°$, the feed rate $F = 2000$ mm/min, and the drawing height equal to $h = 40$ mm. The adoption of a spiral trajectory has been demonstrated to yield superior surface quality compared to traditional contour toolpath (Jeswiet et al., 2005), underscoring its efficacy in achieving desired forming outcomes. To accurately implement this toolpath, we utilized CATIA as a CAD software equipped with an integrated CAM package, enabling seamless generation of coordinates (x, y, z) to guide the forming tool's movements. Figure 2 presents a visual representation of the programmed toolpath, showcasing the prescribed process parameters and the trajectory followed by the forming tool. This graphical depiction provides a clear insight into the planned sequence of movements and aids in understanding how the chosen toolpath influences the deformation process. By employing this approach, we aimed to optimize the forming process and enhance the quality of the formed part, leveraging the benefits afforded by the spiral toolpath strategy. This systematic approach not only facilitates precise control over forming parameters but also contributes to the overall efficiency and reliability of the SPIF process.

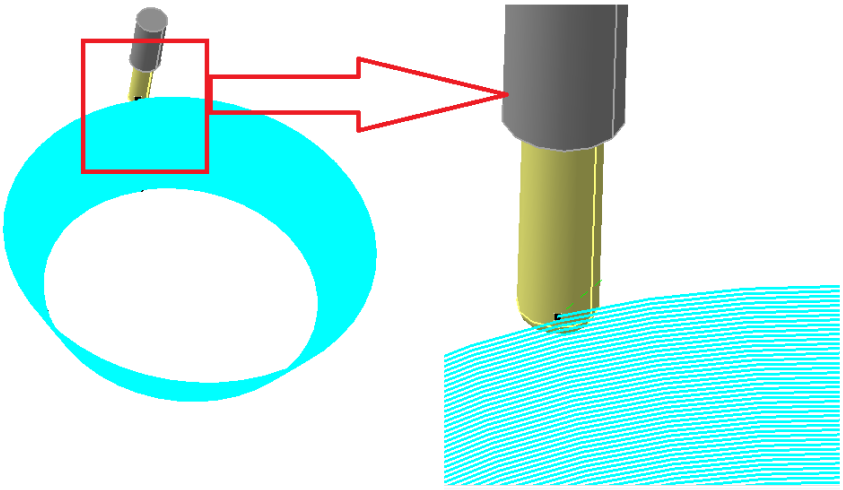

Figure 2. *Spiral toolpath with standard parameters*

4. Numerical modeling of SPIF

A finite element simulation was conducted to assess the single-point incremental sheet metal forming of an aluminum alloy sheet, specifically Al 3003-O. The choice of the Abaqus Explicit package was deliberate, taking into account material nonlinearities and substantial deformation inherent in the process. The sheet is represented as a deformable body with dimensions of 1.2 mm thickness and a 200×200 mm^2 square sheet, while the forming tool and the backing plate are modeled as rigid bodies. A lubrification has been used during the experimental investigation which prove to adopt a friction coefficient $f = 0.1$ to model the interactions between the tools and the sheet at the interface. An assembly model is depicted in Figure 3.

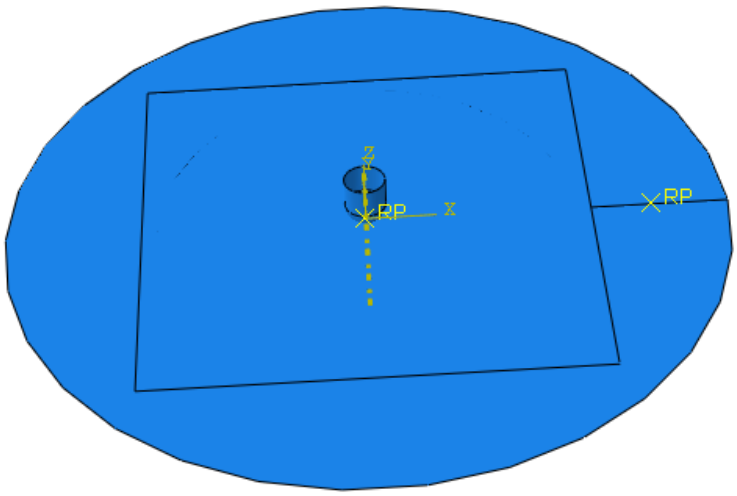

Figure 3. *Assembly model of SPIF process*

4.1. Boundary conditions

Given the non-symmetrical nature of the deformation process, we undertook a comprehensive modeling approach in our simulation. To accurately capture the real-world conditions, the sheet was securely fixed along its edges to replicate practical constraints. In our simulation setup, a controlled displacement was meticulously applied to the forming tool, guiding its movement along the (x, y) plane at each contour, while a specific step depth (Δz) was systematically implemented to govern its downward motion. This approach allowed us to simulate the incremental forming process with precision, mimicking the sequential movements of the forming tool as it gradually shapes the material. To execute these intricate movements, we leveraged the Computer-Aided Manufacturing (CAM) capabilities of CATIA software. The CAM package facilitated the programming of tool movements in the x, y, and z directions, ensuring seamless coordination between the virtual representation of the forming tool and the numerical simulation environment. By employing this integrated approach, we were able to accurately replicate the dynamic interactions between the forming tool and the workpiece, capturing the nuanced complexities inherent in the single-point incremental forming (SPIF) process. This enabled us to generate reliable data and insights into the behavior of forming forces, stress distribution, and deformation patterns, contributing to a deeper understanding of SPIF and its optimization for practical applications.

4.2. Meshing setup

Incremental sheet metal forming processes involve significant deformation and displacement. Hence, a quadrilateral shell element with 4 nodes and 6 degrees of freedom (DOFs) per node, denoted as S4R, was selected for this forming operation. Mesh grid independence was assessed by employing mesh sizes of $m_1 = 1.25\,mm$, $m_2 = 0.75$ mm, and $m_3 = 0.5$ mm across the sheet surface. The relative error between the three meshes was determined, with the difference between m_1 and m_2 assumed to be 6.9%. However, the discrepancy between m_2 and m_3 was approximately 1.5%, indicating that m_2 is sufficiently accurate for subsequent analyses. This choice of mesh size is further supported by Figure 4, illustrates the variation of the Force Vector Sum and its Mean Magnitude with the number of mesh elements.

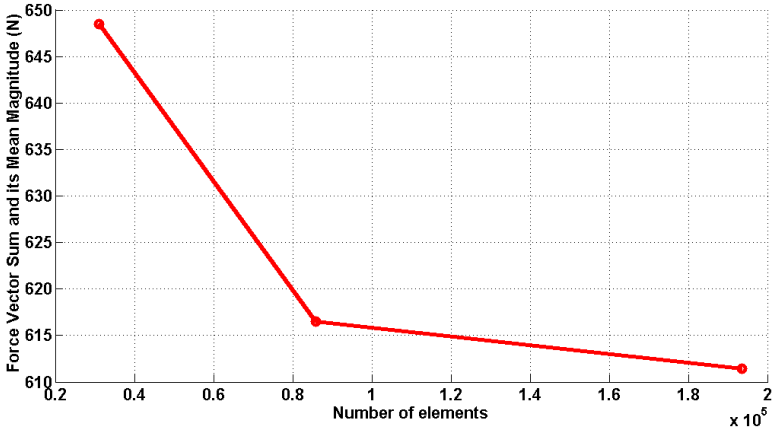

Figure 4. *Results of mesh sensitivity analysis*

5. Results & discussions

Single-point incremental forming (SPIF) is a complex process influenced by various process parameters that have an impact on the forming force, surface quality, and stress distribution. Forming forces F_x, F_y, and F_z were evaluated both numerically and experimentally, following the methodology outlined by Duflou et al. (2007), and are depicted in Figure 5, showing good agreement between the two sets of results. Both graphs exhibit an initial increase in the forming force followed by a plateau, suggesting a constant value until the operation's completion. This behavior is attributed to the mechanical resistance of the part to plastic deformation before reaching the yield point σ_y. While F_x and F_y display similar magnitudes and sinusoidal shapes with a maximum magnitude $F_{max} = 200$ N, the forming force in the z-direction demonstrates a dominant amplitude compared to the other forces. This emphasizes its importance in machine selection for executing the operation.

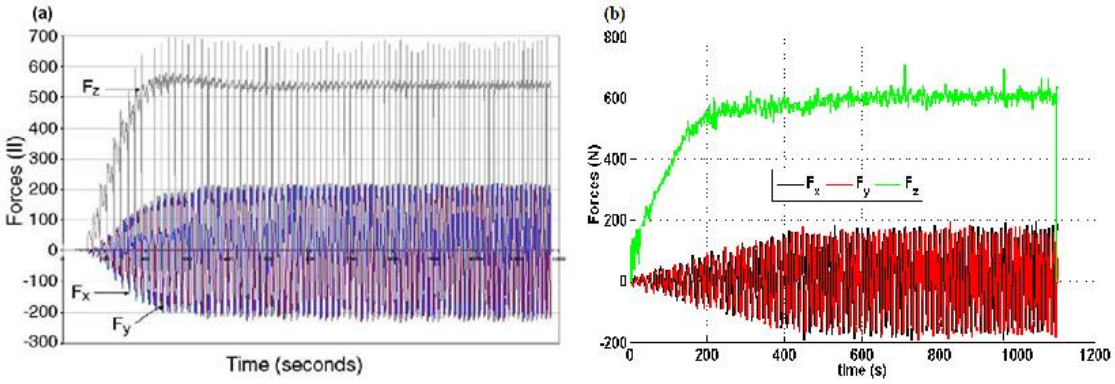

Figure 5. *Experimental and numerical results for the forming forces during SPIF with standards parameters (a) Experimental data: Three force components F_x, F_y, and F_z (Duflou et al., 2007) , (b) numerical data: Three force components F_x, F_y, and F_z*

5.1. Stress distribution

The stress distribution within sheet metal forming processes serves as a critical indicator of the internal stress state within the deformed material. In our research study, we conducted a thorough analysis of stress distribution using, a contour path in the rolling direction parallel to the (y, z) plane on one hand, and a contour path in the transverse direction on the other (Figure 6), with stress curves depicted in Figure 7. A detailed examination of these curves reveals a significant observation: stress levels notably escalate in regions where the forming tool penetrates deeper into the material, particularly reaching a maximum value near the bottom corner compared to other sections along the wall or other parts of the conical shape. This elevation in stress can be attributed to the phenomenon of high thinning, where the material undergoes substantial deformation in response to the forming tool's action. Conversely, stress levels are relatively low at the fixed edges of the sheet, where predominantly bending stress occurs due to the boundary conditions imposed during forming. Additionally, the stress variation exhibits an asymmetric pattern in both rolling and transverse directions, a characteristic that can be attributed to the inherent non-symmetrical nature of the SPIF process. This asymmetry in stress distribution underscores the complex interplay of various factors influencing the deformation process. It's noteworthy that the stress reaches a peak value of 95 MPa and 100 MPa in the 0° and 90° directions, respectively. It is

apparent that the stress magnitude variation along both contour paths is very close, owing to the small difference between the anisotropy coefficients r_0 and r_{90}. This comprehensive analysis of stress distribution sheds light on the intricate mechanics at play during SPIF and provides valuable insights into optimizing process parameters, mitigating material failure risks, and enhancing the overall efficiency and quality of formed components.

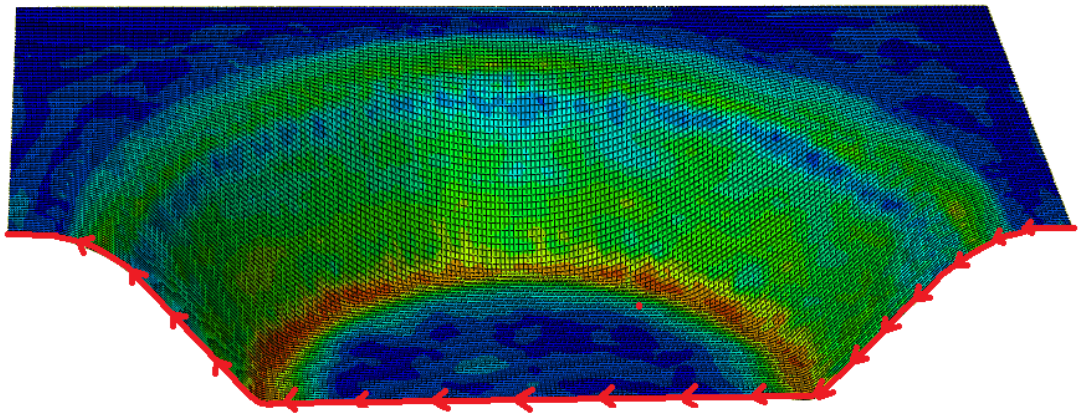

Figure 6. *Path contour along (y, z) plane in the transverse direction*

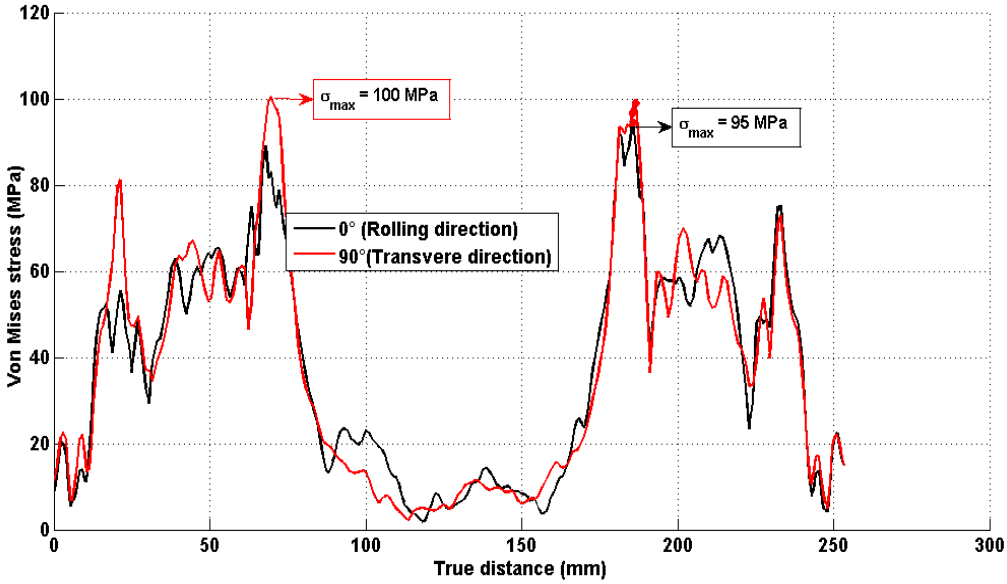

Figure 7. *Stress distribution along the 0° and 90° directions*

6. Conclusions

Throughout this research, numerical modeling using the finite element method was conducted to analyze the behavior of forming forces and stress distribution during single-point incremental forming (SPIF) of aluminum alloy Al 3003-O. The findings revealed significantly higher amplitude values of the forming

force in the out-of-plane direction (F_z) compared to those in the in-plane directions (x, y), which enables it to be crucial for choosing the forming machine and the measrement equipment to perform the forming stage. Despite the geometry's symmetry, the stress distribution exhibited an asymmetric pattern, indicating the non-symmetrical nature of the deformation process.

References

[1] Jeswiet, J., Micari, F., Hirt, G., Bramley, A., Duflou, J., & Allwood, J. (2005). Asymmetric single point incremental forming of sheet metal. *CIRP annals*, *54*(2), 88–114. **https://doi.org/10.1016/S0007-8506(07)60021-3**

[2] Ambrogio, G., Filice, L., & Gagliardi, F. (2012). Formability of lightweight alloys by hot incremental sheet forming. *Materials & Design*, *34*, 501–508. **https://doi.org/10.1016/j.matdes.2011.08.024**

[3] Wang, H., Ye, F., Chen, L., & Li, E. (2017). Sheet metal forming optimization by using surrogate modeling techniques. *Chinese Journal of Mechanical Engineering*, *30*(1), 22–36. **https://doi.org/10.3901/CJME.2016.1020.123**

[4] Hirt, G., Ames, J., Bambach, M., & Kopp, R. (2004). Forming strategies and process modelling for CNC incremental sheet forming. *CIRP Annals*, *53*(1), 203–206. **https://doi.org/10.1016/S0007-8506(07)60679-9**

[5] Filice, L., Fratini, L., & Micari, F. (2002). Analysis of material formability in incremental forming. *CIRP Annals*, *51*(1), 199–202. **https://doi.org/10.1016/S0007-8506(07)61499-1**

[6] Mezher, M. T., Namer, N. S. M., & Nama, S. A. (2018). Numerical and experimental investigation of using lubricant with nano powder additives in SPIF process. *International Journal of Mechanical Engineering and Technology*, *9*(13), 968–977.

[7] Paniti, I., Viharos, Z. J., Harangozó, D., & Najm, S. M. (2020). Experimental and numerical investigation of the single-point incremental forming of aluminium alloy foils. *Acta IMEKO*, *9*(1), 25–31. **https://doi.org/10.21014/acta_imeko.v9i1.750**

[8] Trzepieciński, T., Najm, S. M., Oleksik, V., Vasilca, D., Paniti, I., & Szpunar, M. (2022). Recent developments and future challenges in incremental sheet forming of aluminium and aluminium alloy sheets. *Metals (basel)*, *12*(1), 124. **https://doi.org/10.3390/met12010124**

[9] Li, Y., Lu, H., Daniel, W. J., & Meehan, P. A. (2015). Investigation and optimization of deformation energy and geometric accuracy in the incremental sheet forming process using response surface methodology. *The International Journal of Advanced Manufacturing Technology*, *79*, 2041–2055. **https://doi.org/10.1007/s00170-015-6986-5**

[10] Tisza, M., Kovács, P. Z., & Lukács, Z. (2013). Incremental forming: an innovative process for small batch production. *In Materials Science Forum*, *Trans Tech Pub*, *729*, 85–90. **https://doi.org/10.4028/www.scientific.net/MSF.729.85**

[11] Li, Y., Liu, Z., Daniel, W. J. T., & Meehan, P. A. (2014). Simulation and experimental observations of effect of different contact interfaces on the incremental sheet forming process. *Materials and Manufacturing Processes*, *29*(2), 121–128. **https://doi.org/10.1080/10426914.2013.822977**

[12] Gatea, S., Ou, H., & McCartney, G. (2016). Review on the influence of process parameters in incremental sheet forming. *The International Journal of Advanced Manufacturing Technology* , 87 , 479–499. **https://doi.org/10.1007/s00170-016-8426-6**

[13] Habbachi, M., & Baksa, A. (2024). Numerical modeling and experimental investigation of incremental sheet metal forming of Aluminum Alloy Al 3003-O. In *Journal of Physics: Conference Series* (Vol. 2848, No. 1, p. 012006). IOP Publishing. **https://doi.org/10.1088/1742-6596/2848/1/012006**

[14] Li, J., Li, S., Xie, Z., & Wang, W. (2015). Numerical simulation of incremental sheet forming based on GTN damage model. *The International Journal of Advanced Manufacturing Technology, 81*, 2053–2065. **https://doi.org/10.1007/s00170-015-7333-6**

[15] Duflou, J., Tunckol, Y., Szekeres, A., & Vanherck, P. (2007). Experimental study on force measurements for single point incremental forming. *Journal of Materials Processing Technology, 189*(1-3), 65–72. **https://doi.org/10.1016/j.jmatprotec.2007.01.005**